# Controlled oil/water partitioning of hydrophobic substrates extends the bioanalytical applications of droplet-based microfluidics

Tomas Buryska[†‡#], Michal Vasina[†‡#], Fabrice Gielen[§‖], Pavel Vanacek[†‡], Liisa van Vliet[§], Jan Jezek[⊥], Zdenek Pilat[⊥], Pavel Zemanek[⊥], Jiri Damborsky[†‡], Florian Hollfelder[§], Zbynek Prokop[†‡*]

[#] These authors contributed equally to this work.

[*]Author for correspondence: Zbynek Prokop, zbynek@chemi.muni.cz, +420 54949 6667.

† Loschmidt Laboratories, Department of Experimental Biology and RECETOX, Faculty of Science, Masaryk University, Kamenice 5, 625 00 Brno, Czech Republic

‡ International Clinical Research Center, St. Anne's University Hospital, Pekarska 53, 656 91 Brno, Czech Republic

§ Department of Biochemistry, University of Cambridge, 80 Tennis Court Road, Cambridge CB2 1GA, UK

‖ Living Systems Institute, University of Exeter, Exeter EX4 4QD, UK

⊥ Institute of Scientific Instruments, Czech Academy of Sciences, Kralovopolska 147, 612 64 Brno, Czech Republic

**ABSTRACT:** Functional annotation of novel proteins lags behind the number of sequences discovered by the next-generation sequencing. The throughput of conventional testing methods is far too low compared to sequencing, thus experimental alternatives are needed. Microfluidics offer throughput and reduced sample consumption as a tool to keep up with a sequence-based exploration of protein diversity. The most promising droplet-based systems have a significant limitation: leakage of hydrophobic compounds from water compartments to the carrier prevents their use with hydrophilic reagents. Here, we present a novel approach to substrate delivery into microfluidic droplets and apply it to high-throughput functional characterization of enzymes that convert hydrophobic substrates. Substrate delivery is based on the partitioning of hydrophobic chemicals between the oil and water phases. We applied a controlled distribution of 27 hydrophobic haloalkanes from oil to reaction water droplets to perform substrate specificity screening of eight model enzymes from the haloalkane dehalogenase family. This droplet-on-demand microfluidic system reduces the reaction volume 65,000-times and increases the analysis speed almost 100-fold compared to classical test-tube assay. Additionally, the microfluidic setup enables a convenient analysis of dependences of activity on the temperature in a range 5 to 90 °C for a set of mesophilic and hyper stable enzyme variants. A high correlation between the microfluidic and test-tube data supports the approach robustness. The precision is coupled to considerable throughput of >20,000 reactions per day and will be especially useful for extending the scope of microfluidic applications for high-throughput analysis of reactions including compounds with limited water solubility.

## INTRODUCTION

Advances in sequencing technologies result in the accumulation of vast amounts of sequence information, in most cases lacking functional knowledge of the encoded proteins. A systematic functional characterization of multiple candidates cannot be addressed by conventional approaches, even when automated liquid handling systems are applied because high sample costs and low throughput (typically $<10^4$). Microfluidic technology offers an attractive throughput of up to $10^7$ assays per day and a significant reduction for sample amount requirements.[1] The ultra-high-throughput has been exploited for example in on-chip sorting approaches for directed evolution of proteins is possible at > kHz rates in picoliter volumes.[2–6] Amongst such droplet-based technologies, droplet-on-demand platforms enable the rapid characterization of compound libraries and the acquisition of automated dose-response curves with exquisite control over droplet content and order.[7] The droplets content can be analyzed by diverse analytical methods covering optical microscopy,[8] electrochemical measurements,[9] absorbance[10] and fluorescence detection,[11,12] Raman spectroscopy,[13] mass spectroscopy[14] or electrophoresis.[15] Despite its great potential, droplet microfluidics still faces drawbacks like leakage of hydrophobic compounds,[16] channel wetting and cross-contamination.[17] The leakage of hydrophobic compounds (e.g. substrates, fluorophores, drugs/drug-leads, vitamins) from water compartments to the carrier oil represents one of the major problems and limits the use of these effective analytical systems. The process of extraction of hydrophobic molecules from the water droplet to the oil phase or neighboring droplets can be as fast as a few milliseconds when convection plays a role.[16,18] There is a number of attempts which, however, could only partially prevent the escape of hydrophobic compounds to the oil phase, e.g. addition of bovine serum albumin[17] or sugar molecules,[19] modifications of surfactant[20] or using nanoparticles instead of surfactant.[21]

The leakage of hydrophobic compounds thus remains the major limitation of droplet-based microfluidics.

Here we present a novel approach that addresses the control of hydrophobic compounds in droplet microfluidic systems: the hydrophobic compounds are solubilized in the fluorinated oil phase and delivered to the dispersed aqueous phase by partitioning. At equilibrium, the final concentration of the compound in the water compartments was determined by its oil/buffer partitioning coefficient and the concentration of the compound in the oil phase. We demonstrate the utility of this approach with biochemical characterization of a model enzyme family, haloalkane dehalogenases that converts a wide range of small hydrophobic halogenated alkanes. Specifically, the oil/buffer partitioning coefficients for series of small mono-, di- and tri-halogenated aliphatic hydrocarbons were determined and the oil/buffer distributions used to control the delivery of these hydrophobic compounds into aqueous reaction droplets. Combinatorial analysis of the specific activity of 8 representative haloalkane dehalogenases with a set of 27 representative substrates was performed within 24 hours, which represents a nearly 100-fold reduction in time and a 10,000-fold lower requirement for the total amount of enzyme in comparison to classical test-tube assay.[22] The substrate screening and additional analysis of the temperature optima for a set of mesophilic and hyper stable variants showed high consistency of the microfluidic data with the test-tube measurements.

## MATERIALS AND METHODS

**Materials.** All chemicals used in this study were research grade purity >95% and were purchased from Merck (Merck, USA). The PicoSurf 1 surfactant was purchased from Dolomite (Dolomite, UK). FC40 oil was purchased from 3M (3M, USA). The Portex (Smiths Medical, USA) and TYGON (Saint-Gobain, France) tubing were used in the microfluidic setup. The connectors were purchased from IDEX (IDEX, USA).

**Oil/buffer partitioning of halogenated compounds.** The partition coefficient of the tested halogenated compounds was analyzed by monitoring the distribution in a two-phase system composed by 1 mL HEPES buffer (1 mM, pH 8.0) and 1 mL FC40 oil (3M, USA). The analysis was performed in a screw-capped vial with a magnetic cap at 37 °C. In both phases, the concentration of a particular compound was quantified using the gas chromatograph Trace 1300 (Thermo Scientific, USA) equipped with capillary column TG-SQC (30m x 0.25mm x 0.25µm, Thermo Scientific, USA) and connected to the mass spectrometer ISQ LT Single Quadrupole (Thermo Scientific, USA). The 1 µL of the sample was injected into the split–splitless inlet at 250 °C, with split ratio 1:50. The sample preparation was fully handled by an automatized robotic arm (Pal RTC, CTC analytics, Switzerland). The temperature program was isothermal at 40 °C for 1 min, followed by an increase to 140 °C at 20 °C·min$^{-1}$ and hold for 8 min. The flow of carrier gas (He) was 1 mL·min$^{-1}$. The spectrometer was operated at a SCAN mode (30 to 300 amu). The temperature of the ion source and GC-MS transfer line was 200 °C and 250-300 °C, respectively. The partitioning coefficient was calculated as the logarithm of the compound concentration ratio in fluorinated oil and aqueous buffer using the following formula:

$$\mathrm{Log}P_{\mathrm{oil/buf}} = \log\frac{[\mathrm{compound_{oil}}]}{[\mathrm{compound_{buffer}}]}$$

**Design of microfluidic platform.** The commercial robotic sampler Dropix (Dolomite Microfluidics, UK) and an in-house constructed incubation chamber, a temperature controller and an optical setup for monitoring the biochemical reactions in droplets were assembled (**Figure 1**, **Supporting Figure S1-3**). The droplets were generated by moving vertically the arm with a tubing end between oil and an aqueous sample. Access to up to 24 different samples was reached by horizontally positioning the arm along the rack with samples. Typically, 20 µL of each enzyme sample was loaded into a 24-well rack in the Dropix instrument (Dolomite, UK). An oil bath below the rack was prefilled with FC40 oil with 0.5% PicoSurf 1 surfactant. A fine bore polythene tubing (OD 0.8 mm, ID 0.4 mm, Smith-Medical, UK) was used for the droplet generation and the signal observation. Droplets were generated by a syringe pump (Chemyx, USA) running in the withdraw mode at a flow rate 10 µL·min$^{-1}$. Droplet volume, oil spacing and sample sequence were controlled using the Dropix control software.

**Choice of tubing material**. During the development, it was necessary to find suitable capillary material meeting the following criteria: (i) minimal background signal for the fluorescence detection; (ii) permeability for halogenated substrates through the wall; (iii) relatively low thickness of the capillary wall; and (iv) inner and outer diameter dimensions compatible with the Dropix instrument. We have tested tubing made of polyethylene (PE), polyetheretherketone (PEEK), polytetrafluoroethylene (PTFE), fluorinated ethylene propylene (FEP), perfluoroalkoxy based polymer (PFA) and Tygon. Due to relatively high chemical resistance, very low or no substrate permeability was observed in the cases of FEP, PFA, PEEK and PTFE, therefore we did not use these tubing materials in the following experiments. Higher porosity and lower chemical resistance of tubing materials resulted in the detection of significant substrate concentrations in the oil and aqueous phases for the PE and Tygon tubing. We decided to use the PE tubing in all the following experiments as it had a thinner wall, lower background signal and simpler manipulation.

**Substrate delivery and incubation of the reaction.** The incubation chamber consisted of closed 1.5 mL glass vial in which 20 cm of the tubing was bend in three round loops to prevent droplet squeezing and breakage. The loop went in and out of the vial through a septum with punched holes (**Supporting Figure S2**). The particular halogenated substrate filled in a glass vial passes the capillary wall and then the equilibrium between the carrier oil and aqueous droplets containing an enzyme was reached. The vials with the tubing immersed in the substrate were equilibrated for a minimum of 12 hours prior to the examination. The incubation time can be regulated from 1 to 10 min based on the applied flow rates. The description of an alternative approach suitable for substrate delivery of hydrophobic compounds that do not penetrate the tubing wall is provided in the **Supporting Methods**.

**Design of temperature control.** To control the temperature of the incubation chamber, we manufactured a copper block with a drilled hole for bringing a thermocouple into direct contact

with the vial (**Supporting Figure S4**). Heating and cooling were achieved by a Peltier element glued to the copper block and controlled by the manufacturer's computer software (Meerstetter, Switzerland). Excess heat was removed by a heat pipe connected to a cooler with a fan. The system working temperature ranged from 5 °C to 90 °C, with 0.1 ºC accuracy. The temperature on the surface of the glass vial was validated using infrared thermal imaging. Nevertheless, the system was always equilibrated at a set temperature for a minimum time of 15 minutes. Heat transfer in the droplets on a short distance is a fast phenomenon and the droplet reaches target temperature upon arrival to the vial placed in the heated block in less than 1 s.[23]

**The activity assay, signal acquisition and processing.** We employed pH-based fluorescence assay for monitoring the enzymatic activity in the microfluidic droplets. Small changes in the pH can be observed in simple systems consisting of a weak buffer, e.g. HEPES, and a complementary fluorescent indicator, e.g. 8-hydroxypyrene-1,3,6-trisulfonic acid (HPTS).[24,25] Reaction progress was analyzed as an end-point measurement recorded after passing through the incubation chamber. The optical fiber was locked in a perpendicular position towards the capillary in an in-house fabricated black acetal cube. The excitation light is transferred to the sample only in the central part of the optical fiber, whereas the emission light was collected by all surrounding fibers. Such an optical bundle setup significantly reduces noise from the excitation light and increases the amount of the collected light where the excitation source has enough power. Optical excitation was achieved by a blue laser (450 nm, 12V, 200mW, PRC) focused by a spherical lens into the multimode optical fiber Y-bundle (SQS, Czech Republic). The excitation wavelength was filtered on a dichroic mirror with a cut-off at 490 nm (ThorLabs, Germany). The analogue signal was collected by a Si-detector (ThorLabs, Germany), converted to a digital signal by Ni-DAQ 6009 module (National Instruments, USA) and processed by LabView 12 (National Instruments, USA). The raw signal was processed by a droplet detection script written in MATLAB 2017b (Mathworks, USA). The signal analysis script is provided in the Supporting Information (**Supporting Script**).

The assembled system was calibrated for the monitoring of the pH change using 2 mM, 1.0 mM, 0.5 mM and 0.25 mM HCl. The calibration was performed in the HEPES buffer (1 mM HEPES, 20 mM $Na_2SO_4$, pH 8.0) with 50 μM HPTS as the fluorescence indicator. A further decrease in the acid concentration was not distinguishable from the buffer solution (**Figure 1C and 1D**). The calibration consisted of a continuous sequence of the buffer, HCl/HBr in a descending concentration and a buffer, where each solution was loaded as 10 droplets of 150 nL volume with 300 nL oil spacing. The standard deviation among droplets with the same solution was typically lower than 1 %. The calibration sequence was performed whenever a new tubing was used.

**Robotic activity screening.** Specific activities of LinB towards the set of 27 halogenated substrates were analyzed using a Hamilton MICROLAB STARlet robot (Hamilton Robotics, Switzerland). The reactions were performed in 2 mL glass vials containing 1 mL of 100 mM glycine buffer, pH 8.6 and 1 μL of the halogenated substrate at 37 °C. The reaction was initiated by addition of the enzyme. The progress of the reaction was monitored by periodically withdrawing samples from the reaction mixture and immediately mixing these samples with 35% (v/v) nitric acid to terminate the reaction. The release of the halide ion product was analyzed spectrophotometrically using an end-point assay developed by Iwasaki and co-workers.[26] The dehalogenation activities were quantified by the rate of product formation over time.

**Data analysis and statistics.** Specific activities for the 8 HLDs and 27 halogenated substrates measured by the microfluidic and robotic method were compared to the data analyzed by classical test-tube method taken from the work by Koudelakova *et al*.[22] Pearson and Spearman correlation coefficients were calculated for each substrate comparing test-tube and microfluidics data (**Supporting Table S6**). The relationship between the enzymes and clustering to the substrate specificity groups was studied by Principal Component Analysis (PCA) using Statistica 13 (TIBCO, USA). A detailed explanation of the PCA has been described previously.[22] Briefly, the raw data were log-transformed and weighted relative to the individual enzyme's activity. Each value needed to be incremented by 1 to avoid the logarithm of zero values. The resulting values were then divided by the sum of values for a particular enzyme and weighted values were estimated. These transformed data were used to calculate principal components and the components explaining the highest variability in the data were then plotted for identification of substrate specificity groups.

## RESULTS

We adopted classical droplet-based microfluidics to the analysis of reactions including compounds with limited water solubility by delivering these chemicals to the reaction droplet via an oil-water interface. At equilibrium, the final concentration of the compounds in the water compartments was determined by its oil/buffer partitioning coefficient and the concentration of the substrate in the oil phase. A brief description of the steps applied to screen activity of set of enzymes to a single hydrophobic substrate is the following: (i) loading of the calibration and enzyme solutions in the sample holder rack, (ii) starting of the pump, (iii) measurement of droplet data for calibration sequence and (iv) running and measurement of droplet trains containing the enzymatic samples separated by buffer droplets, stopping the flow and changing to the next substrate. The whole procedure took approximately 30 minutes for a single substrate and all enzymes tested. Generated droplet sequence traveled through an incubation chamber filled with a particular halogenated compound. The substrate penetrated through the capillary walls and equilibrates between the oil and aqueous droplets where reacted with the enzymes. After the incubation, an optical signal resulted from the enzymatic reaction was detected with a fiber optics coupled to a laser source exciting pH-sensitive fluorophore (HPTS) in a droplet and concurrently transfers the emitted light to the detector (**Figure 1A**).

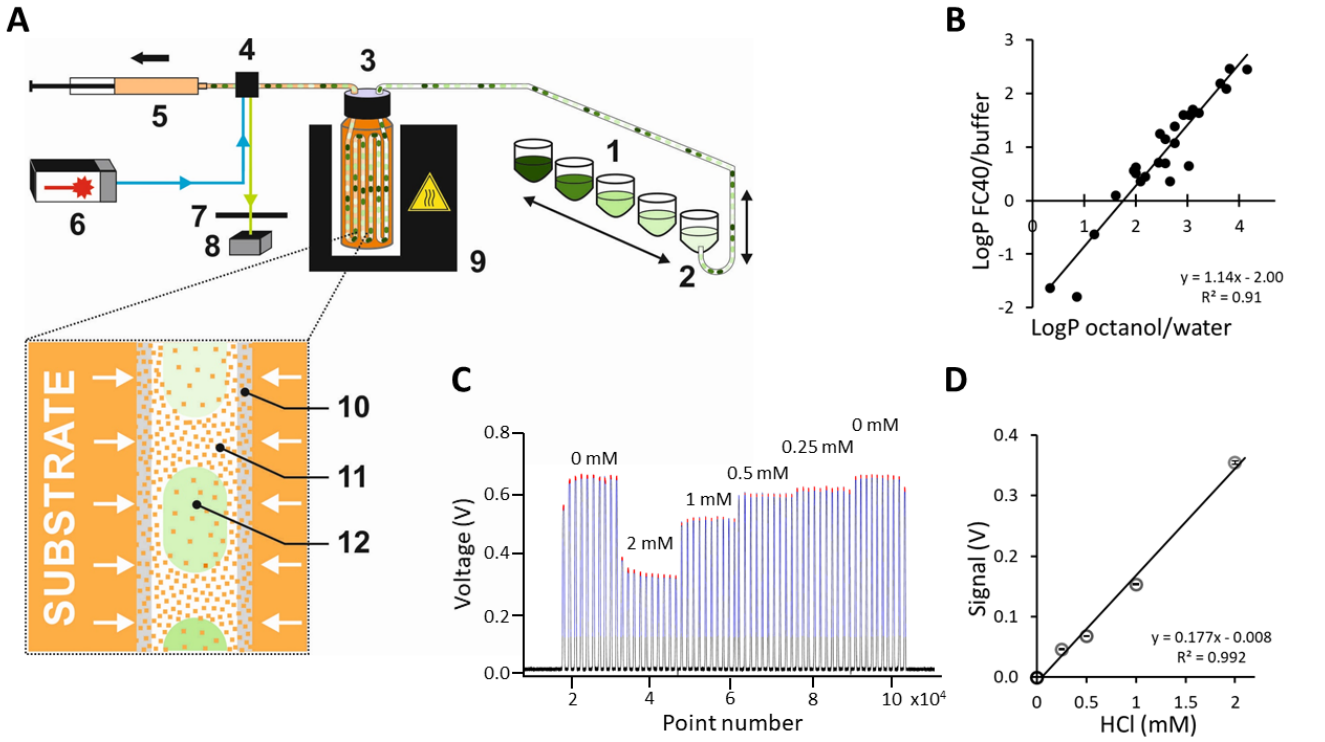


**Figure 1: Capillary–based microfluidic platform.** (**A**) A scheme of the platform. Aqueous samples are loaded in a bottomless rack (1), which is placed at the top of an oil bath of the Dropix instrument. Droplets are generated by a vertical movement of a hook (2) with a polythene tubing up and down between the oil bath and the rack with samples. Different enzyme samples are exchanged by a horizontal movement of the hook. Polythene tubing connected to a syringe pump in a withdrawal mode (5) is going through an incubation chamber (3) and a black Delrin (DuPont) cube (4) serving as a detection point. Excitation light from a laser source (6) is brought to the tubing inside the detection cube. The reflected emission light is collected after passing through a dichroic mirror (7) at a photodetector (8). The temperature is controlled by a custom-made heating block (9). The schematic view of substrates delivery (bottom left). A substrate (orange) passes through the tubing wall (10), dissolves in a carrier oil (11) and finally reaches aqueous droplets (12) by oil/water partitioning. The hydrophobic compound (orange) penetrates through the capillary wall (grey) and equilibrates between the oil (white) and aqueous droplets containing enzyme samples (shades of green). (**B**) The equilibrium distribution of substrates between oil and aqueous phases. The FC40/HEPES buffer partitioning coefficients analyzed by gas chromatography for 25 halogenated compounds compared to octanol/water partitioning coefficients retrieved from the ChemSpider (http://www.chemspider.com). (**C**) A raw data record from the calibration sequence. The blue color represents a signal above the threshold (black color) used for droplet detection. The red color represents a signal peak averaged during the droplet analysis. Dilution series of a hydrochloric acid run in ten repetitions was used for the calibration (**D**).

**Analysis of partitioning and substrate delivery.** The equilibrium distribution between the fluorinated oil FC40 and a buffer solution (1 mM HEPES buffer, pH 8.0) was studied for a set of halogenated compounds by monitoring the concentration in both of the immiscible phases using gas chromatography (**Supporting Table S1**). The specific FC40/HEPES buffer partition coefficients ($LogP_{oil/buf}$) ranged from -1.79 to 2.47, however, most of the compounds prefer the fluorinated oil phase with $LogP_{oil/buf} > 0$. Partitioning coefficients $LogP_{oil/buf}$ correlates well with the partition coefficients for octanol/water ($LogP_{oct/wat}$) retrieved from the ChemSpider database ($R^2 = 0.91$) (**Figure 1B**).The relationship between $LogP_{oilbuf}$ and $LogP_{oct/wat}$ indicates a reduced solubility of the tested compounds in FC40 in comparison to octanol which is consistent with previous studies assuming reduced solubility of short halogenated compounds in fluorinated oils.[27,28] Still, the concentrations reached several to ten´s mM in a fluorinated oil (**Supporting Figure S2B**) and thanks to lowering of $LogP_{oil/buf}$ all the tested compounds approached a concentration in water phase comparable with conditions achieved in a classical test-tube assay where the compounds are solubilized directly in an aqueous phase. The relationship between $LogP_{oil/buf}$ and $LogP_{oct/wat}$ was used for estimation of the equilibrium distribution of the tested compound in a two-phase microfluidic system but can also be applied for a prediction of the behavior of other chemically-related compounds. Next, we estimated the kinetics of the substrate distribution. We calculated the diffusion times of 1,2-dibromoethane in $H_2O$ and FC40 for a distance of 1 µm under static conditions using the methodology described previously elsewhere (**Supporting Methods**).[16] The calculated times 0.6 ms and 1.5 ms for $H_2O$ and FC40, respectively, indicate rapid equilibration during compounds delivery with no significant limitations for the kinetics of the biochemical reaction, incubated on a time scale of minutes.

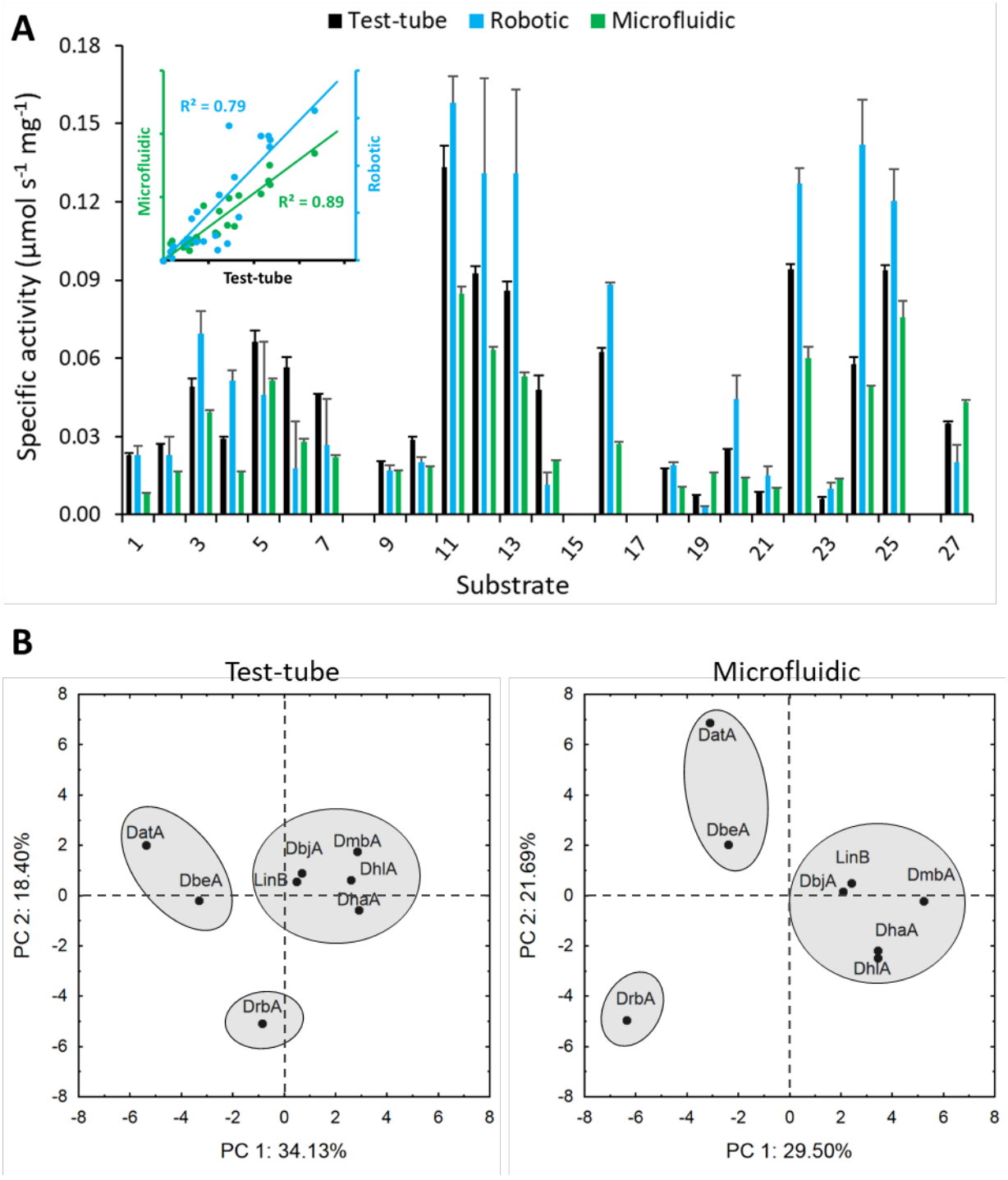


**Figure 2: Analysis of substrate specificity.** (**A**) Comparison of the substrate specificity profiles of HLD LinB determined by using a test-tube method (black), a liquid handling robot (blue) and capillary-based microfluidics (green). A positive activity for 23 out of 27 tested substrates was observed in all cases. A complete list of substrates and their specific activities is provided in Supporting information. The error bars represent standard errors to the data based on ten droplets average signal. Specific activities for the test-tube measurement were taken from Koudelakova *et al*.[22] The error bar for test-tube data is calculated from three repetitions. The inset shows the correlation for the specific activities of the test-tube, robotic (blue) and capillary-based microfluidics data (green). (**B**) Comparison of the specificity profiles of 8 different enzymes using Principal Component Analysis of the transformed specific activities determined with 27 halogenated compounds. The score plots presenting the data from the test-tube and the capillary-based microfluidics. The score plots are two-dimensional projections of two factors covering the highest variability of the data. HLDs cluster into three substrate specificity groups visualized using the ovals.

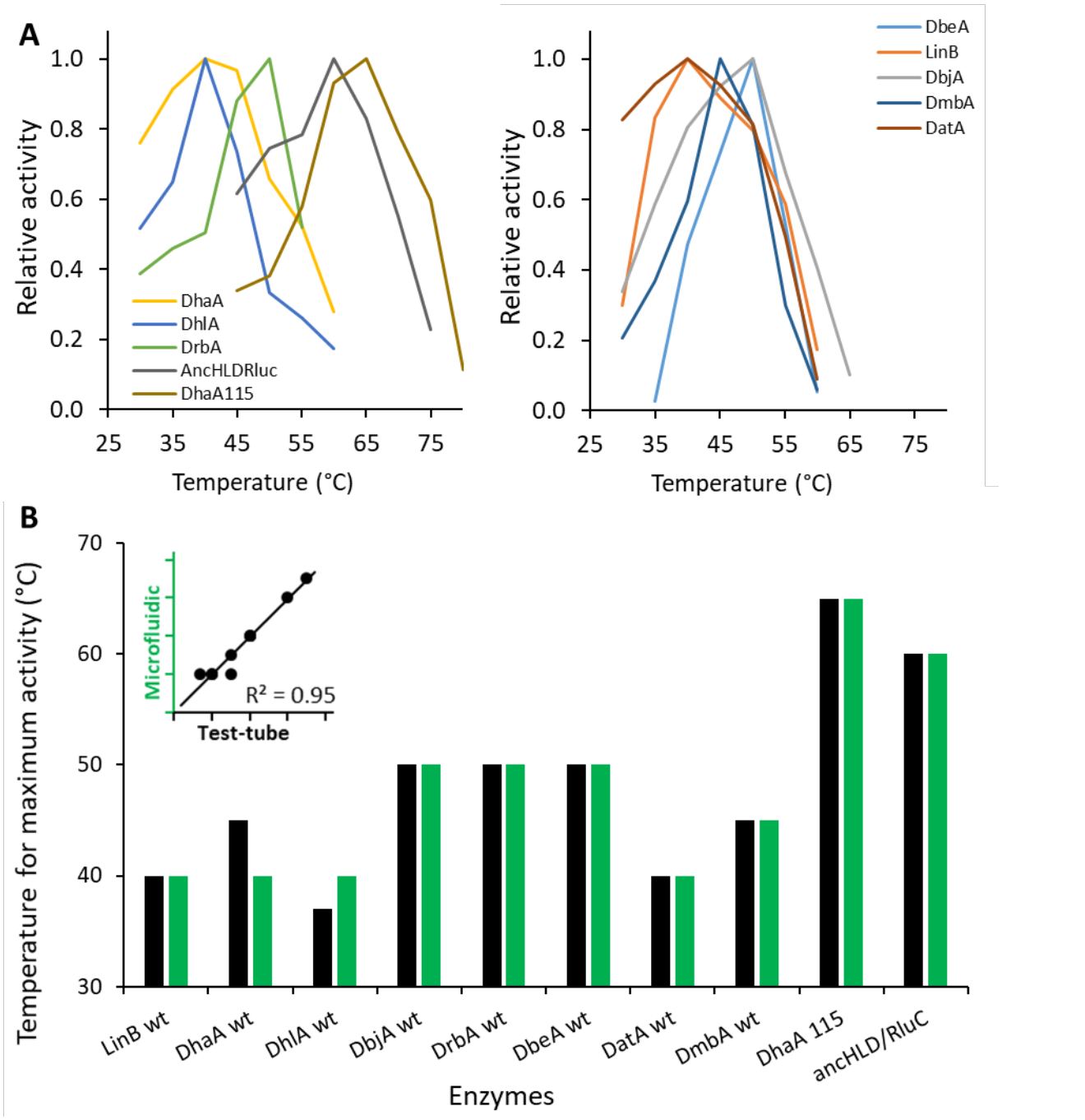


**Figure 3: Evaluation of temperature profiles.** (**A**) Relative activities of 10 haloalkane dehalogenases at different temperature. For clarity, the data were split into two parts. Each activity point is based on an average of 10 droplets. The data are relativized towards the highest activity of a particular enzyme. (**B**) Comparison of enzyme temperature optima determined by a test-tube method (black) and capillary-based microfluidics (green). Temperature optima determined by classical test-tube approach were extracted from the study of Koudelakova *et al.*[32] LinB, DmbA, DhlA, DbeA, DatA, DrbA, DbjA, and DhaA are the wild type enzymes, DhaA115 is a hyper-stable variant engineered by computational protein design[33] and ancHLD-RLuC is a hyper-stable reconstructed ancestral protein of HLDs and *Renilla* luciferase. The inset shows the correlation between test-tube and microfluidic data.

The compound transfer and equilibration is expected to be even faster during the flow regime of operation due to convection.[29] The transfer of the compounds to the oil and water phase has been tested experimentally in a microfluidic system (**Supporting Figure S2**).

We studied the concentration of compounds in FC40 and aqueous droplets and the dependency on varying the aspiration rate from 5 $\mu L \cdot min^{-1}$ to 20 $\mu L \cdot min^{-1}$ that resulted in droplet residence times from 1 to 5 minutes. The different flow rates (for different

incubation time) did not significantly affect the final concentration of the compounds in both phases supporting the rapid equilibration estimated from diffusion times. The concentrations of the compounds tested were based on solubility and ranged from 3 to 60 mM in the FC40 and from 0.4 to 20 mM in the buffer. Prior to each experiment, the system was calibrated by a dilution series of acid for the signal response (**Figure 1C and 1D**). Droplet monodispersity was estimated from the intrinsic time spent in the detector and was less than 7% (**Supporting Figure S3**).

**Comparison of microfluidic, robotic and test-tube method.** Specific activities of the model enzyme, haloalkane dehalogenase LinB from *Sphingobium japonicum* UT26,[30] with a standard set of 27 representative substrates were measured using the microfluidic system and a liquid handling robot. Both the microfluidic and robotic data sets were compared with previously reported values obtained by test-tube biochemical assay (**Supporting Table S2**).[22] A positive enzymatic activity was observed for 23 substrates, while 4 substrates were not converted. This result was consistent throughout all the three data sets, test-tube, robotic and microfluidic (**Figure 2A**). Quantitative analysis showed a strong correlation of the test-tube measurement with robotic and microfluidic analysis with the Pearson coefficients 0.89 and 0.94, respectively (**Figure 2A inset**). A slight shift was observed for absolute values, the robotic data exhibit a 23 % increase while microfluidic data a 37 % decrease of averaged activity values in comparison to the data measured by classical test-tube assay. Generally, the test-tube method requires about 2-3 weeks to measure the substrate specificity profile for a single enzyme. The employment of robotic liquid handling sped up the process about 8–fold.[31] However, it still required relatively large amounts of samples (**Supporting Table S3**). The microfluidic screening of 8 model enzymes with 27 substrates was achieved within 24 hours, which speeds up the process nearly 100 times in comparison to the test-tube method. The reaction volume scaled down to the 150 nL, representing about a 65 000-fold reduction in the sample volume requirement.

**Method validation in a combinatorial specificity screening of eight model enzymes.** Next, we applied the microfluidic system for combinatorial screening of the activity of eight HLDs towards a set of 27 representative substrates (**Supporting Table S4 and Figure S5**). The microfluidic data were statistically analyzed by using Principal Component Analysis (PCA) and compared with data obtained by classical test-tube assay reported previously by Koudelakova *et al.* (**Figure 2B**).[22] The PCA analysis of both the test-tube and microfluidic analyses identically clustered the enzymes to three substrate specificity groups. The principal components 1 and 2 covered variances of 52 and 51% variances in the data for the test-tube and microfluidic approaches, respectively. Both analyses yield closely similar coordinates for the same enzymes. Larger deviations were detected only for DrbA and DatA, both representing enzymes with very low specific activities close to the detection limits of the assay (**Supporting Figure S6**).

**Analysis of temperature optima.** The temperature optimum was determined for the set of eight HLDs previously used for the specificity screening, all showing mesophilic characteristic with temperature optimum between 40 °C to 50 °C.[32] For better comparison, the set of tested enzymes was additionally enriched by two HLDs variants with significantly improved thermal stability: (i) hyperstableDhaA115 engineered by using FireProt computational protein design[33] and (ii) hyper-stable ancHLD-RLuc, which is a reconstructed ancestral protein of HLDs and *Renilla luciferase* (**Figure 3A**).[34] In the experiment, 1,2-dibromoethane served as a substrate and the reactions were measured by the 5-degree increment from 30°C to 80 °C. The temperature optima obtained by microfluidic approach showed an excellent correlation ($R^2$ = 0.95) with test-tube data previously reported for the tested enzyme variants (**Figure 3B inset**). The difference observed for DhaA wt can be caused by almost identical values between 40 and 45°C. In the case of DhlA wt, the observed 40°C is slightly above the reported 37°C.

## CONCLUSIONS

A droplet has been often considered as a self-contained reactor flowing in the carrier phase.[29] However, droplets are not isolated objects and leakage of hydrophobic compounds to an oil phase can be only partially prevented.[20,35] We have shown that hydrophobic compounds can be distributed from an oil phase (substrate stock) into aqueous droplets. This overcomes the problem of containment of hydrophobic compounds in droplets in the classical droplet microfluidics, where compounds with an octanol-water partition coefficient larger than zero escape from water reaction droplets and disperse in fluorinated oil. Instead of treating droplets as isolated compartments in the carrier phase, we deliver hydrophobic compounds via a water-oil interface by the means of reaching equilibrium between the two phases. Substrate loading via an oil phase enables an analysis of hydrophobic compounds, which would not be possible using the classical approach where all reactants are present and delivered via aqueous solutions. Our analysis of short halocarbons revealed a high correlation ($R^2$ = 0.91) of oil-buffer partitioning with the logPs reported in standard octanol-water conditions.

The novel substrate delivery route opened the possibility of adopting classical microfluidics to the analysis of reactions including compounds with limited water solubility. We demonstrated the utility of this approach during the combinatorial screening of the activity of the model enzymes family, haloalkane dehalogenases, with a representative set of hydrophobic substrates. The biochemical data obtained using the droplet-based microfluidic system were critically compared with the test-tube and robotic analyses. The quantitative comparison showed a high correlation between test-tube and microfluidic measurements with the correlation coefficients 0.94 and 0.98 for substrate specificity and temperature optimum data, respectively. The presented platform will find use in screening campaigns for rapid profiling of activity, substrate specificity and temperature profiles from psychrophilic to thermophilic enzymes. The presented method uses a fluorescence probe to monitor a change of pH universal for numerous enzyme families that are important for industrial or medical applications (e.g., carboxylesterases, acetylcholinesterases, ureases, lipases, proteases, pyruvate kinases, glycoside hydrolases or glucose oxidases), without requirements for specific fluorogenic substrates. Additionally, the presented detection approach is not limited to the fluorescence only and can easily be applied also in the absorbance mode as demonstrated previously[7,36,37].

## ASSOCIATED CONTENT

### Supporting Information

Technical details on the alternative substrate delivery process are described. Throughput and sample consumption of test-tube, robotic and microfluidic approach is compared. Data used in the estimation of the partitioning coefficients. Concentrations of selected substrates in aqueous and oil phase are provided. The table used for comparison of raw specific activities on LinB. Raw data used in the statistical analyses. Raw signal analysis script for extraction of droplet signal in MATLAB is also provided. Finally, more detailed platform schematics is described.

## AUTHOR INFORMATION

### Corresponding Author

* Zbynek Prokop, zbynek@chemi.muni.cz, +420 54949 6667.

### Author Contributions

TB designed and conducted the experiments, analyzed and interpreted the data and wrote the manuscript. MV designed and conducted the experiments, analyzed the data and wrote the manuscript. FG and LV designed the experiments. PV conducted experiments and interpreted the data. JJ, ZPi and PZ contributed to the system development. FH and JD wrote the manuscript. ZPr designed the microfluidics setups and experiments, interpreted the data and wrote the manuscript.

## ACKNOWLEDGEMENT

This research is supported by the Czech Science Foundation (GA16-07965S), infrastructure was supported by the Ministry of Education Youths and Sports of the Czech Republic (LQ1605 LO1214, CZ.02.1.01/0.0/0.0/16_026/0008451, CZ.02.1.01/0.0/0.0/16_019/0000868, LM2015051, CZ.02.1.01/0.0/0.0/16_013/0001761) and the European Commission (720776, CZ.1.05/2.1.00/01.0017). FH is an ERC Advanced Investigator (grant no. 695669). We acknowledge Zdenek Janicek for the help with the acquisition of the robotic data and David Damborsky for his help with the estimation of partitioning coefficients.

## REFERENCES

(1) Dittrich, P. S.; Manz, A. Lab-on-a-Chip: Microfluidics in Drug Discovery. *Nat. Rev. Drug Discov.* **2006**, *5* (3), 210–218.

(2) Agresti, J. J.; Antipov, E.; Abate, A. R.; Ahn, K.; Rowat, A. C.; Baret, J.; Marquez, M.; Klibanov, A. M.; Griffiths, A. D.; Weitz, D. a. Ultrahigh-Throughput Screening in Drop-Based Microfluidics for Directed Evolution. *Proc. Natl. Acad. Sci. U. S. A.* **2010**, *107* (9), 4004–4009.

(3) Kintses, B.; Hein, C.; Mohamed, M. F.; Fischlechner, M.; Courtois, F.; Lainé, C.; Hollfelder, F. Picoliter Cell Lysate Assays in Microfluidic Droplet Compartments for Directed Enzyme Evolution. *Chem. Biol.* **2012**, *19* (8), 1001–1009.

(4) Colin, P.-Y.; Kintses, B.; Gielen, F.; Miton, C. M.; Fischer, G.; Mohamed, M. F.; Hyvönen, M.; Morgavi, D. P.; Janssen, D. B.; Hollfelder, F. Ultrahigh-Throughput Discovery of Promiscuous Enzymes by Picodroplet Functional Metagenomics. *Nat. Commun.* **2015**, *6*, 10008.

(5) Mair, P.; Gielen, F.; Hollfelder, F. Exploring Sequence Space in Search of Functional Enzymes Using Microfluidic Droplets. *Curr. Opin. Chem. Biol.* **2017**, *37*, 137–144.

(6) Obexer, R.; Godina, A.; Garrabou, X.; Mittl, P. R. E.; Baker, D.; Griffiths, A. D.; Hilvert, D. Emergence of a Catalytic Tetrad during Evolution of a Highly Active Artificial Aldolase. *Nat. Chem.* **2016**, *9*, 50–56.

(7) Gielen, F.; van Vliet, L.; Koprowski, B. T.; Devenish, S. R. A.; Fischlechner, M.; Edel, J. B.; Niu, X.; DeMello, A. J.; Hollfelder, F. A Fully Unsupervised Compartment-on-Demand Platform for Precise Nanoliter Assays of Time-Dependent Steady-State Enzyme Kinetics and Inhibition. *Anal. Chem.* **2013**, *85* (9), 4761–4769.

(8) Fradet, E.; Bayer, C.; Hollfelder, F.; Baroud, C. N. Measuring Fast and Slow Enzyme Kinetics in Stationary Droplets. *Anal. Chem.* **2015**, *87* (23), 11915–11922.

(9) Han, Z.; Li, W.; Huang, Y.; Zheng, B. Measuring Rapid Enzymatic Kinetics by Electrochemical Method in Droplet-Based Microfluidic Devices with Pneumatic Valves. *Anal. Chem.* **2009**, *81* (14), 5840–5845.

(10) Gielen, F.; Hours, R.; Emond, S.; Fischlechner, M.; Schell, U.; Hollfelder, F. Ultrahigh-Throughput-Directed Enzyme Evolution by Absorbance-Activated Droplet Sorting (AADS). *Proc. Natl. Acad. Sci. U. S. A.* **2016**, *113* (47), E7383–E7389.

(11) Olguin, L. F.; Askew, S. E.; O'Donoghue, A. C.; Hollfelder, F. Efficient Catalytic Promiscuity in an Enzyme Superfamily: An Arylsulfatase Shows a Rate Acceleration of 10(13) for Phosphate Monoester Hydrolysis. *J. Am. Chem. Soc.* **2008**, *130* (49), 16547–16555.

(12) Clausell-Tormos, J.; Lieber, D.; Baret, J.-C.; El-Harrak, A.; Miller, O. J.; Frenz, L.; Blouwolff, J.; Humphry, K. J.; Köster, S.; Duan, H.; et al. Droplet-Based Microfluidic Platforms for the Encapsulation and Screening of Mammalian Cells and Multicellular Organisms. *Chem. Biol.* **2008**, *15* (5), 427–437.

(13) Kim, H. S.; Waqued, S. C.; Nodurft, D. T.; Devarenne, T. P.; Yakovlev, V. V; Han, A. Raman Spectroscopy Compatible PDMS Droplet Microfluidic Culture and Analysis Platform towards On-Chip Lipidomics. *Analyst* **2017**, *142* (7), 1054–1060.

(14) Fidalgo, L.; Whyte, G. Coupling Microdroplet Microreactors with Mass Spectrometry: Reading the Contents of Single Droplets Online. *Angew. Chemie Int. Ed.* **2009**, 3665–3668.

(15) Roper, M. G.; Shackman, J. G.; Dahlgren, G. M.; Kennedy, R. T. Microfluidic Chip for Continuous Monitoring of Hormone Secretion from Live Cells Using an Electrophoresis-Based Immunoassay. *Anal. Chem.* **2003**, *75* (18), 4711–4717. https://doi.org/10.1021/AC0346813.

(16) Chen, Y.; Wijaya Gani, A.; Tang, S. K. Y. Characterization of Sensitivity and Specificity in Leaky Droplet-Based Assays. *Lab Chip* **2012**, *12* (23), 5093–5103. https://doi.org/10.1039/c2lc40624a.

(17) Courtois, F.; Olguin, L. F.; Whyte, G.; Theberge, A. B.; Huck, W. T. S.; Hollfelder, F.; Abell, C. Controlling the Retention of Small Molecules in Emulsion Microdroplets for Use in Cell-Based Assays. *Anal. Chem.* **2009**, *81* (8), 3008–3016.

(18) Skhiri, Y.; Gruner, P.; Semin, B.; Brosseau, Q.; Pekin, D.; Mazutis, L.; Goust, V.; Kleinschmidt, F.; El Harrak, A.; Hutchison, J. B.; et al. Dynamics of Molecular Transport by Surfactants in Emulsions. *Soft Matter* **2012**, *8* (41), 10618–10627.

(19) Sandoz, P. A.; Chung, A. J.; Weaver, W. M.; Di Carlo, D. Sugar Additives Improve Signal Fidelity for Implementing Two-Phase Resorufin-Based Enzyme Immunoassays. *Langmuir* **2014**, *30* (23), 6637–6643.

(20) Baret, J. C. Surfactants in Droplet-Based Microfluidics. *Lab Chip* **2011**, *12* (3), 422–433. https://doi.org/10.1039/c1lc20582j.

(21) Pan, M.; Rosenfeld, L.; Kim, M.; Xu, M.; Lin, E.; Derda, R.; Tang, S. K. Y. Fluorinated Pickering Emulsions Impede Interfacial Transport and Form Rigid Interface for the Growth of Anchorage-Dependent Cells. *ACS Appl. Mater. Interfaces* **2014**, *6* (23), 21446–21453.

(22) Koudelakova, T.; Chovancova, E.; Brezovsky, J.; Monincova, M.; Fortova, A.; Jarkovsky, J.; Damborsky, J. Substrate Specificity of Haloalkane Dehalogenases. *Biochem. J.* **2011**, *2410* (2), 345–354.

(23) Lignos, I.; Stavrakis, S.; Nedelcu, G.; Protesescu, L.; deMello, A. J.; Kovalenko, M. V. Synthesis of Cesium Lead Halide Perovskite Nanocrystals in a Droplet-Based Microfluidic Platform: Fast Parametric Space Mapping. *Nano Lett.* **2016**, *16* (3), 1869–1877.

(24) Nevolova, S.; Manaskova, E.; Mazurenko, S.; Damborsky, J.; Prokop, Z. Development of Fluorescent Assay for Monitoring of Dehalogenase Activity. *Biotechnol. J.* **2018**, 1800144.

(25) Gielen, F.; Butz, M.; Rees, E. J.; Erdelyi, M.; Moschetti, T.; Hyvönen, M.; Edel, J. B.; Kaminski, C. F.; Hollfelder, F. Quantitative Affinity Determination by Fluorescence Anisotropy Measurements of Individual Nanoliter Droplets. *Anal. Chem.* **2017**, *89* (2), 1092–1101.

(26) Iwasaki, I.; Utsumi, S.; Ozawa, T. New Colorimetric Determination of Chloride Using Mercuric Thiocyanate and Ferric Ion. *Bull. Chem. Soc. Jpn.* **1952**, *25* (3), 226.
(27) Scott, R. L. The Solubility of Fluorocarbons. *J. Am. Chem. Soc.* **1948**, *70* (12), 4090–4093.
(28) Gruner, P.; Riechers, B.; Semin, B.; Lim, J.; Johnston, A.; Short, K.; Baret, J. C. Controlling Molecular Transport in Minimal Emulsions. *Nat. Commun.* **2016**, *7*, 10392.
(29) Song, H.; Chen, D. L.; Ismagilov, R. F. Reactions in Droplets in Microfluidic Channels. *Angew. Chemie Int. Ed.* **2006**, *45* (44), 7336–7356.
(30) Nagata, Y.; Hynkova, K.; Damborsky, J.; Takagi, M. Construction and Characterization of Histidine-Tagged Haloalkane Dehalogenase (LinB) of a New Substrate Class from a Gamma-Hexachlorocyclohexane-Degrading Bacterium, Sphingomonas Paucimobilis UT26. *Protein Expr. Purif.* **1999**, *17* (2), 299–304.
(31) Vanacek, P.; Sebestova, E.; Babkova, P.; Bidmanova, S.; Daniel, L.; Dvorak, P.; Stepankova, V.; Chaloupkova, R.; Brezovsky, J.; Prokop, Z.; et al. Exploration of Enzyme Diversity by Integrating Bioinformatics with Expression Analysis and Biochemical Characterization. *ACS Catal.* **2018**, *8* (3), 2402–2412.
(32) Koudelakova, T.; Bidmanova, S.; Dvorak, P.; Pavelka, A.; Chaloupkova, R.; Prokop, Z.; Damborsky, J. Haloalkane Dehalogenases: Biotechnological Applications. *Biotechnol. J.* **2013**, *8* (1), 32–45.
(33) Bednar, D.; Beerens, K.; Sebestova, E.; Bendl, J.; Khare, S.; Chaloupkova, R.; Prokop, Z.; Brezovsky, J.; Baker, D.; Damborsky, J. FireProt: Energy- and Evolution-Based Computational Design of Thermostable Multiple-Point Mutants. *PLOS Comput. Biol.* **2015**, *11* (11), e1004556.
(34) Chaloupkova, R.; Liskova, V.; Toul, M.; Markova, K.; Sebestova, E.; Hernychova, L.; Marek, M.; Pinto, G. P.; Pluskal, D.; Waterman, J.; et al. Light-Emitting Dehalogenases: Reconstruction of Multifunctional Biocatalysts. *ACS Catal.* **2019**, *9* (6), 4810–4823.
(35) Gruner, P.; Riechers, B.; Semin, B.; Lim, J.; Johnston, A.; Short, K.; Baret, J. C. Controlling Molecular Transport in Minimal Emulsions. *Nat. Commun.* **2016**, *7*, 10392.
(36) Gielen, F.; Buryska, T.; Vliet, L. Van; Butz, M.; Damborsky, J.; Prokop, Z.; Hollfelder, F. Interfacing Microwells with Nanoliter Compartments: A Sampler Generating High-Resolution Concentration Gradients for Quantitative Biochemical Analyses in Droplets. *Anal. Chem.* **2014**, *87* (1), 624–632.
(37) Yang, T.; Stavrakis, S.; deMello, A. A High-Sensitivity, Integrated Absorbance and Fluorescence Detection Scheme for Probing Picoliter-Volume Droplets in Segmented Flows. *Anal. Chem.* **2017**, *89* (23), 12880–12887

FOR TOC ONLY